

FULL PAPER

Control of snake robots with switching constraints: trajectory tracking with moving obstacle

Motoyasu Tanaka^{a*} and Fumitoshi Matsuno^b

^a*The University of Electro-Communications, 1-5-1 Chofugaoka, Chofu, Tokyo, Japan;*

^b*Kyoto University, Kyotodaigaku-Katsura, Nishikyo-ku, Kyoto, Japan*

(v1.0 released January 20XX)

We propose control of a snake robot that can switch lifting parts dynamically according to kinematics. Snakes lift parts of their body and dynamically switch lifting parts during locomotion: e.g., sinus-lifting and sidewinding motions. These characteristic types of snake locomotion are used for rapid and efficient movement across a sandy surface. However, optimal motion of a robot would not necessarily be the same as that of a real snake as the features of a robot's body are different from those of a real snake. We derived a mathematical model and designed a controller for the three-dimensional motion of a snake robot on a two-dimensional plane. Our aim was to accomplish effective locomotion by selecting parts of the body to be lifted and parts to remain in contact with the ground. We derived the kinematic model with switching constraints by introducing a discrete mode number. Next, we proposed a control strategy for trajectory tracking with switching constraints to decrease cost function, and to satisfy the conditions of static stability. In this paper, we introduced a cost function related to avoidance of the singularity and the moving obstacle. Simulations and experiments demonstrated the effectiveness of the proposed controller and switching constraints.

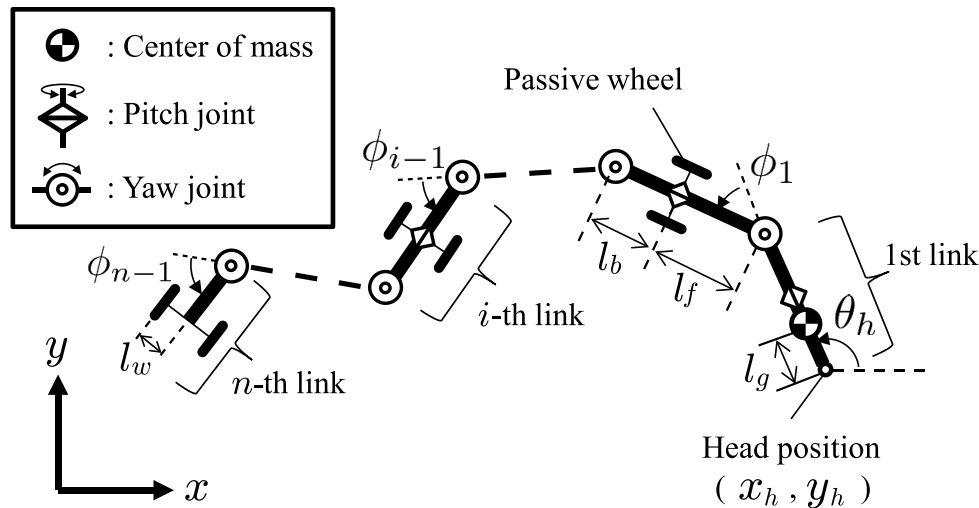
Keywords: snake robot; trajectory tracking; hybrid system; switching constraints; kinematics;

1. Introduction

Snake robots can realize various gaits of snakes and their slim bodies make them useful for the inspection of pipelines and disaster sites [1][2]. Recent studies have proposed snake robots and their locomotion: e.g., there have been studies on obstacle-aided locomotion [3][4], adaptive collision avoidance [5], helical rolling locomotion [6], decentralized control [7], and optimizing coordinates for locomotion [8]. Hirose modeled a snake using a wheeled link mechanism with no side slip and proposed a *serpenoid curve*, which is the most common form of snake locomotion [9]. This paper treats a snake robot based on a wheeled link mechanism (wheeled snake robot) as the controlled object.

Sinus-lifting and sidewinding are forms of locomotion unique to snakes. The sinus-lifting motion is used for rapid movement, while sidewinding is a characteristic locomotion of desert snakes for moving across a sandy surface. Both sinus-lifting and sidewinding locomotion require the snake to lift some parts of its body and to switch these parts dynamically. Burdick derived a three-dimensional kinematic model using the backbone curve and considered the sidewinding locomotion [10]. Hatton analyzed the stability of the sidewinding locomotion on a slope [11]. Ma derived a model considering Coulomb friction for the interaction with the environment and compared the efficiency of serpentine locomotion with that of sinus-lifting locomotion [12]. In these studies, body shape and grounded parts were determined by imitating the motion of a real

*Corresponding author. Email: mtanaka@uec.ac.jp

Figure 1. An n -link snake robot.

snake. Conversely, Shigeta and Tsuda considered the relationship between proposed dynamic manipulability and sinus-lifting motion [13][14]. Lipkin designed various gaits for snake robots inspired by biology and based on empirical experience [15]. Gong proposed the steering method of the sidewinding locomotion [16]. Yamada proposed a steering method by superposition of a pedal wave and a steering wave and investigated the conditions for suitable steering curvature [17]. In these studies, there was no discussion of the automatic control of the snake robot for three-dimensional motions, such as sinus-lifting and sidewinding locomotions. The changes in lifting parts must be considered as a control problem and must be determined adaptively for the various types of effective locomotion of snake robots.

A hybrid system is a dynamic system involving both continuous and discrete dynamics [18][19]. The snake robot with consideration of the switching of lifting parts of its body can be modeled as a hybrid system. A dynamic model was proposed with switching lifting parts of the body of the snake robot along with comparison of the sinus-lifting motion and the optimal switching pattern [20][21]. However, these studies did not consider autonomous control for the desired trajectory as the body shape was a serpenoid curve.

Our goal is to realize effective locomotion of snake robots by switching lifting parts dynamically without regard to locomotion patterns of real snakes. This paper presents the trajectory tracking controller of snake robots that accomplishes sub-tasks using kinematic redundancy and the switching of lifting parts. We select singularity avoidance and moving obstacle avoidance of the body as sub-tasks. Previous methods for the obstacle avoidance of snake robots were to change the path of the robot's head [22–25]. The locomotion achieved by the controller proposed in this paper is a novel effective locomotion because it tracks the motion of the robot's head for an arbitrary trajectory and ensures the body avoids a moving obstacle. We derive the kinematic model of the motion of the snake robot using switching constraints, design the controller to accomplish trajectory tracking, and propose a method for the selection of constraints and switching conditions to ensure static stability and singularity avoidance of the robot. In this paper, we introduce a cost function related to the avoidance of a singularity and a moving obstacle. Simulations and experiments were carried out to determine the effectiveness of the proposed controller and switching constraints.

2. Model

We consider an n link wheeled snake robot as shown in Figure 1. A link comprises a pitch rotational joint and a pair of passive wheels mounted coaxially, and is connected to another

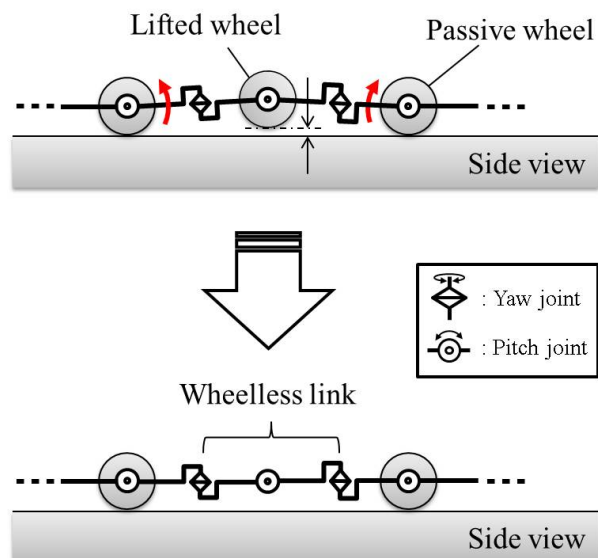


Figure 2. Lifting links and wheelless links.

link via a yaw rotational joint. All wheels are passive and all joints are active. We assume that a passive wheel does not slide in the sideways direction and the environment is flat. l_f is the distance from the anterior end of the link to the wheel axis, l_b is the distance from the posterior end of the link to the wheel axis, l_w is the distance from the center line of a link to the center of a wheel, and l_g is the distance from the anterior end of the link to the center of gravity of the link. The length of the link is $(l_f + l_b)$. The lifting links of the snake robot are regarded as wheelless links of the two-dimensional snake robot, and the grounded links are regarded as the wheeled links (Figure 2). That is, we model the lifting motion of the snake in three-dimensional space by switching the wheeled link to the wheelless link in the two-dimensional motion. We assume that the time required to lift and ground wheels is infinitesimal. Moreover, we assume that the motion of pitch joints does not affect the motion of the position and attitude of the robot's head and links because we set that the desired value of pitch angles is a minute value and the dynamic influence of the motion of pitch joints is small.

2.1 Snake robot

Let $\boldsymbol{\psi} = [\psi_1, \dots, \psi_{n-1}]^T$ be the pitch joint angles of each link and we assume that $\boldsymbol{\psi} \simeq \mathbf{0}$ because we consider the motion of the snake robot on a two-dimensional plane. Let $\boldsymbol{w} = [x_h, y_h, \theta_h]^T$ be the position and attitude of the snake head, $\boldsymbol{\phi} = [\phi_1, \dots, \phi_{n-1}]^T$ be the yaw joint angles of the links, and $\boldsymbol{q} = [\boldsymbol{w}^T, \boldsymbol{\phi}^T]^T$ be generalized coordinates. It is necessary to remove the passive wheel of the head link to control the position and attitude of the snake head at the same time [26]. If the head link is wheelless and other links are wheeled, the kinematic equation of snake robots can be written as

$$A(\boldsymbol{q})\dot{\boldsymbol{w}} = B(\boldsymbol{q})\dot{\boldsymbol{\phi}}. \quad (1)$$

Then, let the “ i -th mode” be the condition in which the i -th constraint condition of the snake robot is satisfied and N_m be the number of modes. In the i -th mode, the constraint condition that m_i (j_1, \dots, j_{m_i} -th) links are wheelless is satisfied, and the kinematic equation of the i -th mode can be written as

$$\tilde{A}_i \dot{\boldsymbol{w}} = \tilde{B}_i \boldsymbol{u} \quad (i = 1, \dots, N_m), \quad (2)$$

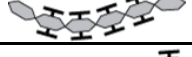
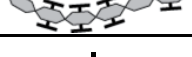
| Mode | Constraint situation | Kinematic equation |
|--------|---|---|
| Mode 1 |  | $\tilde{A}_1 \dot{\mathbf{w}} = \tilde{B}_1 \mathbf{u}$ |
| Mode 2 |  | $\tilde{A}_2 \dot{\mathbf{w}} = \tilde{B}_2 \mathbf{u}$ |
| Mode 3 |  | $\tilde{A}_3 \dot{\mathbf{w}} = \tilde{B}_3 \mathbf{u}$ |
| ⋮ | ⋮ | ⋮ |

Figure 3. Modes and kinematic equations in the case $n = 6$.

where $\tilde{A}_i \in \mathbf{R}^{(n-m_i) \times 3}$ and $\tilde{B}_i \in \mathbf{R}^{(n-m_i) \times (n-1)}$ are matrices whose $(j_2 - 1), \dots, (j_{m_i} - 1)$ -th row vectors are eliminated from the matrices A and B in (1), and $\mathbf{u} = \dot{\boldsymbol{\phi}}$. If $(n - m_i) \geq 3$ is satisfied, the system (2) becomes redundancy controllable [26]. Figure 3 shows an example of modes and kinematic equations in the case $n = 6$.

2.2 Snake robot with switching constraints

Changes in the constraints of the snake robot are because of the active motion of the robot and changes in the environment. In this paper, we consider the active change of constraints by the robot itself. Let ΔT be the switching time period. The system of the snake robot with switching constraints is then expressed as

$$\begin{aligned} \tilde{A}_{\sigma(t)} \dot{\mathbf{w}} &= \tilde{B}_{\sigma(t)} \mathbf{u} \\ \sigma(t) &= \sigma_k, \quad \forall t \in [t_k, t_{k+1}) \end{aligned} \quad (3)$$

where $\sigma \in M$ is the discrete mode number, $M = \{1, 2, \dots, N_m\}$, and $t_k = k\Delta T (k = 0, 1, 2, \dots)$ is the switching time. Figure 4 shows the relationship between σ and time. The mode σ switches at $t = t_k$ instantaneously and holds the mode number at $t_k \leq t < t_{k+1}$ as shown in Figure 4.

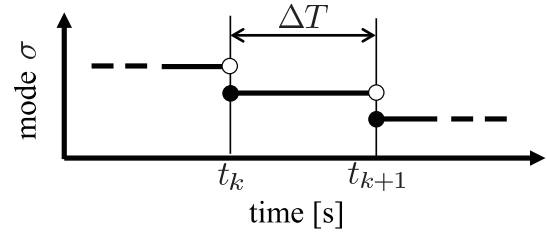
By considering that the first link is wheelless and $n - m_\sigma \geq 3$, the total number of modes N_m is obtained as the following equation.

$$\begin{aligned} N_m &= {}_{n-1}C_{n-1} + {}_{n-1}C_{n-2} + \dots + {}_{n-1}C_3 \\ &= \sum_{j=3}^{n-1} {}_{n-1}C_j \end{aligned} \quad (4)$$

where ${}_iC_j$ is the number of combinations from i to j and ${}_iC_j = \frac{i!}{j!(i-j)!}$. The first link is wheelless and the robot can select whether each of other links is wheeled or wheelless. (4) is the number of combinations of selecting wheeled or wheelless links. In (4), for example, ${}_{n-1}C_{n-1}$ and ${}_{n-1}C_3$ are the number of combinations in the case that the links from the second to n -th are wheeled and in the case that three links are wheeled, respectively. For example, $N_m = 16$ if $n = 6$, and $N_m = 99$ if $n = 8$.

3. Controller design

Snake robots can effectively search narrow spaces. In such environments, snake robots are remotely controlled using information obtained by sensors on the robot, e.g., cameras and laser range finders. Generally, the sensors are set on the head of the robot and the operator controls the robot by indicating the desired direction of the head [27, 28]. Thus, we set the main control

Figure 4. Relationship between σ and time.

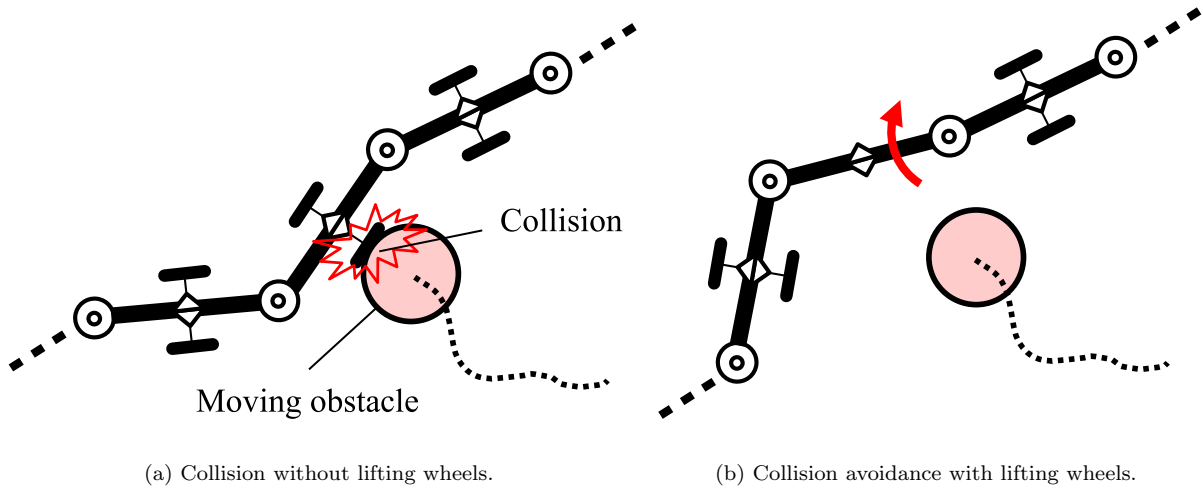


Figure 5. Moving obstacle and the robot.

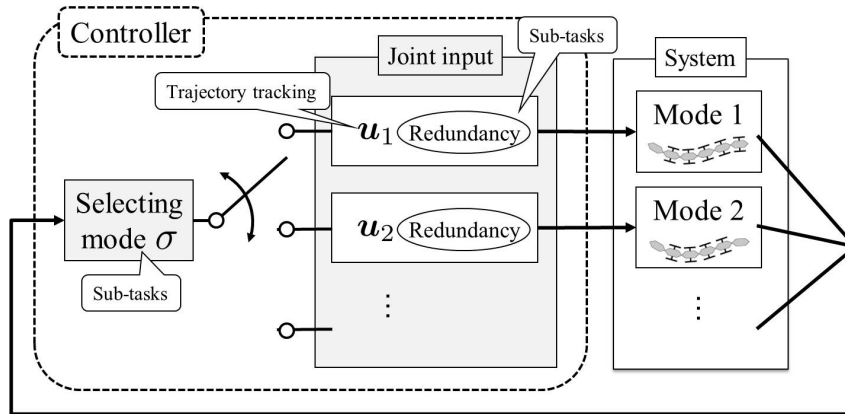


Figure 6. Control strategy.

objective as the trajectory tracking of the head.

Next, we consider the sub control objective. It is necessary for the snake robot to avoid a singular configuration where all the passive wheels are either parallel or in an arc shape [29]. We found that introduction of links without wheels made the robot a kinematically redundant system and the robot could avoid a singularity using redundancy [26]. Hence, we set one of the sub control objectives as singularity avoidance. Furthermore, the robot in this paper can locomote with more freely because the system not only has kinematic redundancy but can also switch modes to realize an additional degree of freedom. Thus, we consider the body avoiding a moving obstacle as shown in Figure 5. In the case without switching modes, it is possible that a link collides with the obstacle as shown in Figure 5(a) because the link has non-holonomic constraints of the wheels and the link can not move to avoid the collision freely. By contrast, the link can move freely to avoid the collision by lifting wheels of the link if the robot can switch the mode as shown Figure 5(b). The switching of modes is effective in avoiding a moving obstacle. We therefore set the additional sub control objective as the avoidance of a moving obstacle.

It is necessary to design the joint input $\mathbf{u}(t)$ and the mode $\sigma(t)$ in (3). Let the main control objective be the trajectory tracking of \mathbf{w} . Let sub control objectives be the avoidance of a singularity and a moving obstacle. The control strategy is shown in Figure 6. The controller consists of the joint input and the selection of the mode. The joint input is the joint angular velocity that rotates the joint of the robot. The selection of the mode σ relates to a constraint

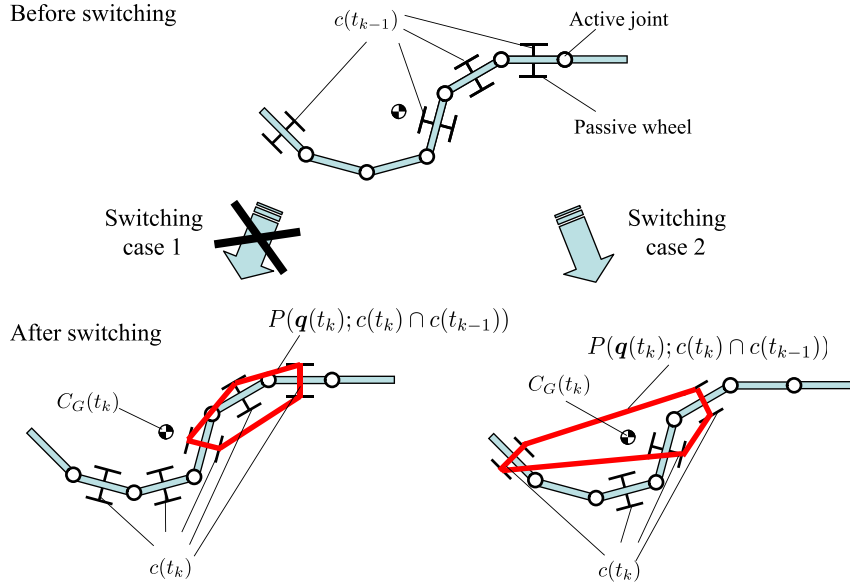


Figure 7. Switching condition (10).

condition of the wheels. The joint input \mathbf{u} is like a parallel distributed controller for each mode. \mathbf{u} involves an element attributed to the redundancy of the robot because the snake robot becomes a redundant system if wheelless links are introduced [26]. In this paper, \mathbf{u} without redundancy is designed to achieve the main control objective, and the redundancy in \mathbf{u} and the mode σ are determined to achieve the sub control objectives.

3.1 Design of input \mathbf{u}

We consider a decrease in the value of the cost function $V(\mathbf{q})$ as sub control objectives (sub-tasks). In system (3) we set the input \mathbf{u} as

$$\begin{aligned} \mathbf{u}(t) &= \mathbf{u}_{\sigma(t)} \\ &= \tilde{B}_{\sigma}^{\dagger} \tilde{A}_{\sigma} \{ \dot{\mathbf{w}}_d - K(\mathbf{w} - \mathbf{w}_d) \} + (I - \tilde{B}_{\sigma}^{\dagger} \tilde{B}_{\sigma}) k_n \boldsymbol{\eta} \end{aligned} \quad (5)$$

where \mathbf{u}_{σ} is the input for the σ -th mode, $\tilde{B}_{\sigma}^{\dagger}$ is a pseudo inverse matrix of \tilde{B}_{σ} , $\boldsymbol{\eta} = (\partial V / \partial \boldsymbol{\phi})^T = [\partial V / \partial \phi_1, \dots, \partial V / \partial \phi_{n-1}]^T$ is the gradient of the cost function $V(\mathbf{q})$, and \mathbf{w}_d is a desired value of \mathbf{w} , $K > 0$ is a feedback gain, and k_n is a gain for sub-tasks. By substituting (5) in (3), the closed-loop system is expressed as

$$\tilde{A}_{\sigma} \{ (\dot{\mathbf{w}} - \dot{\mathbf{w}}_d) + K(\mathbf{w} - \mathbf{w}_d) \} = \mathbf{0}. \quad (6)$$

If the matrix \tilde{A}_{σ} is of full column rank (i.e., the robot is not the singular configuration), the uniqueness of the solution is guaranteed. The solution of (6) is given as

$$(\dot{\mathbf{w}} - \dot{\mathbf{w}}_d) + K(\mathbf{w} - \mathbf{w}_d) = \mathbf{0} \quad (7)$$

and \mathbf{w} converges to the desired trajectory \mathbf{w}_d . Note that (7) is independent of the mode σ . The state variable \mathbf{w} to be controlled converges on its desired vector \mathbf{w}_d exponentially without depending on the switching constraints unless the robot becomes the singular configuration.

The second term on the right hand side of (5) belongs to the null space of matrix \tilde{B}_{σ} , and

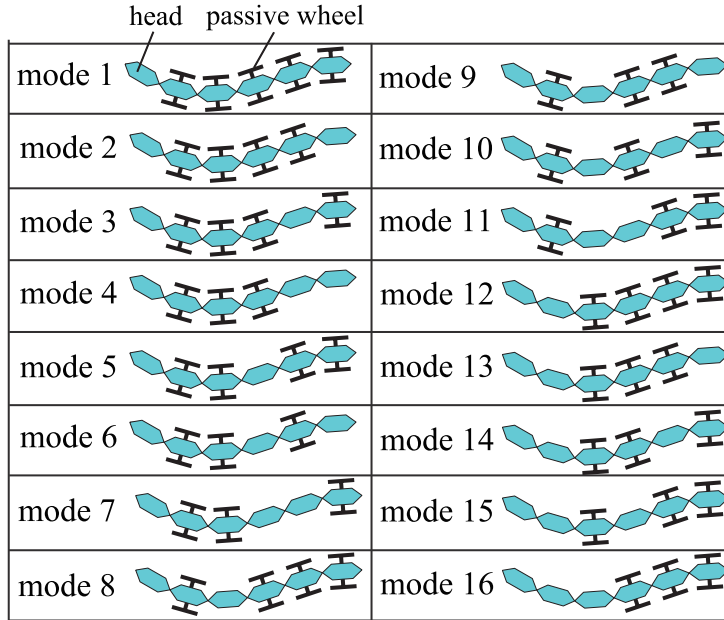


Figure 8. Constraint situations and modes.

expresses the kinematic redundancy. The derivative of V is expressed as

$$\begin{aligned}
 \dot{V}(\mathbf{q}) &= \frac{\partial V}{\partial \mathbf{w}} \dot{\mathbf{w}} + \frac{\partial V}{\partial \phi} \dot{\phi} \\
 &= \frac{\partial V}{\partial \mathbf{w}} \dot{\mathbf{w}} + \frac{\partial V}{\partial \phi} \mathbf{u} \\
 &= \frac{\partial V}{\partial \mathbf{w}} \dot{\mathbf{w}} + \boldsymbol{\eta}^T \tilde{B}_\sigma^\dagger \tilde{A}_\sigma \{ \dot{\mathbf{w}}_d - K(\mathbf{w} - \mathbf{w}_d) \} + \boldsymbol{\eta}^T (I - \tilde{B}_\sigma^\dagger \tilde{B}_\sigma) k_n \boldsymbol{\eta}.
 \end{aligned} \tag{8}$$

By setting $k_n < 0$, the third term on the right of (8) becomes negative semidefinite because $I - \tilde{B}_\sigma^\dagger \tilde{B}_\sigma \geq 0$ [30] and contributes to decrease the cost function V . Thus, the second term of the input (5) can contribute to decrease the cost function V .

3.2 Cost function

Sub-tasks are the avoidance of a singularity and moving obstacles. If the robot is in singular configuration, $\det(\tilde{A}_\sigma^T \tilde{A}_\sigma)$ becomes zero. The robot needs to satisfy $\det(\tilde{A}_\sigma^T \tilde{A}_\sigma) > 0$ to avoid the singular configuration [26]. We assume that the position of the moving obstacle is given and set the cost function V as

$$V(\mathbf{q}) = a \left(\sum_{i=1}^n \frac{1}{d_i} \right) + b \frac{1}{\det(\tilde{A}_\sigma^T \tilde{A}_\sigma)} \tag{9}$$

where d_i is the distance between the center position of the i -th link and the center position of the obstacle (x_{ob}, y_{ob}) , and $a > 0$ and $b > 0$ are weight constants. If the values of d_i and $\det(\tilde{A}_\sigma^T \tilde{A}_\sigma)$ are large, the value of V becomes small. The robot can move to avoid the singular configuration and the collision with the obstacle if the robot moves to decrease V .

3.3 Condition for switching constraints

We consider the condition for static stable locomotion considering the effects of switching modes. At $t = t_k$, let $c(t_k)$ be the set of grounded links, $C_G(t_k)$ be the center of gravity of the whole body of the snake robot, and $P(\mathbf{q}(t_k); c(t_k))$ be the supporting polygon area constructed by the passive wheels of the grounded links. We introduce the conditions

$$C_G(t_k) \in P(\mathbf{q}(t_k); c(t_k) \cap c(t_{k-1})), \quad (10)$$

$$\hat{C}_G(t) \in P(\hat{\mathbf{q}}(t); c(t_k)), \quad t_k \leq t < t_{k+1}, \quad (11)$$

where \hat{C}_G is the estimate value of C_G using the estimate value $\hat{\mathbf{q}}$ of \mathbf{q} that is calculated according to (5) and the solution of (7). The condition (10) means that the center of gravity of the robot is contained in the supporting polygon constructed by the common grounded links ($c(t_k) \cap c(t_{k-1})$) before and after switching. Figure 7 shows examples of condition (10). The snake robot does not satisfy condition (10) in switching case 1 but does satisfy the condition in switching case 2. Condition (11) means that the snake robot is statically stable during $t_k \leq t < t_{k+1}$. The snake robot is ensured the static stability of the gait, and can avoid impractical switching: e.g., switching where all grounded links are switched to lifted links or vice versa by introducing conditions (10) and (11).

However, the snake robot needs to avoid the singular configuration. If \tilde{A}_σ is of row full rank, the snake robot does not have the singular configuration. Therefore, it is necessary to satisfy the condition

$$\hat{k}(t) > c_s, \quad t_k \leq t < t_{k+1}, \quad (12)$$

where $k(t) = \det(\tilde{A}_{\sigma(t)}^T \tilde{A}_{\sigma(t)})$, c_s is a minimal positive value, and \hat{k} is the estimate value of k using $\hat{\mathbf{q}}$.

3.4 Selection of mode by designing σ

Considering conditions (10), (11) and (12), we formulate the decrease in V as a finite time optimal control problem at $t = t_k$:

$$\begin{aligned} \min_{\sigma} \quad & \int_{t_k}^{t_{k+1}} V(\hat{\mathbf{q}}) dt \\ \text{subject to} \quad & \text{Eqs.(10), (11) and (12),} \end{aligned} \quad (13)$$

where $\hat{\mathbf{q}}$ is the estimate vector of \mathbf{q} , and σ_k is the optimal mode that attains the minimum value of (13). σ_k is calculated by a full search of all combinations of switching mode. Based on the fixed mode, the robot calculates the input using (5) and the real-time obstacle's position measured by sensors. This means that the robot attempts to avoid the collision with the obstacle as far as possible in the current mode σ_k . However, when the robot designs σ by the selection of the mode according to (13), the robot calculates the cost function using the obstacle's position $(x_{ob}(t_k), y_{ob}(t_k))$ at $t = t_k$ as the position at $t_k \leq t \leq t_{k+1}$. The robot has the potential to select an unsuitable mode if the obstacle moves quickly because the obstacle's position is treated as a constant. If the obstacle's motion is predicted, the robot can select a more suitable mode by applying the predicted position to (13). We assume that the speed of the obstacle is not high, and this paper does not predict the obstacle's motion to simplify the problem.

The optimal control problem (13) is solved at $t = t_k$ and σ_k is selected as $\sigma(t)$ at $t < t_{k+1}$. The optimal problem (13) can not be proved to be solvable. However, if the robot has many links, there are many modes. Therefore, there is a reasonable possibility that (13) is solvable.

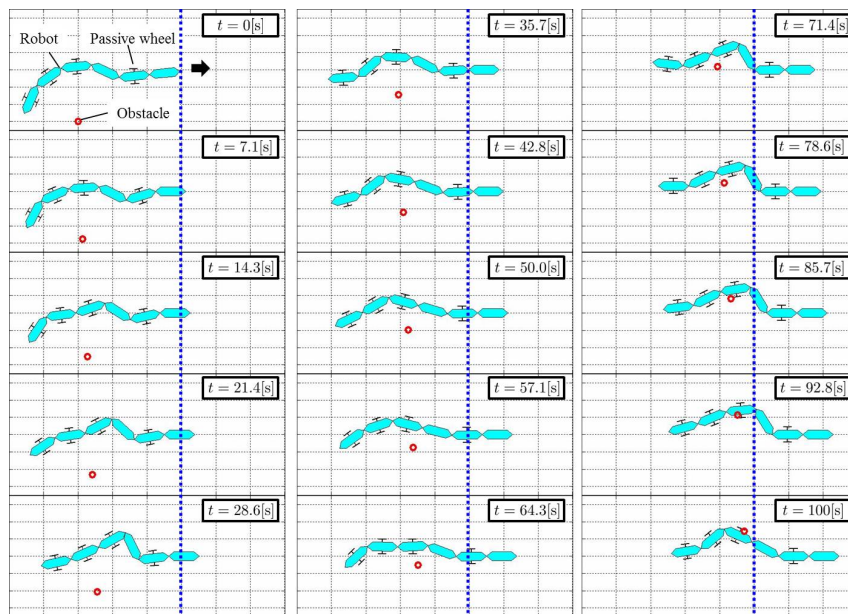


Figure 9. Motion of the robot without switching in simulation.

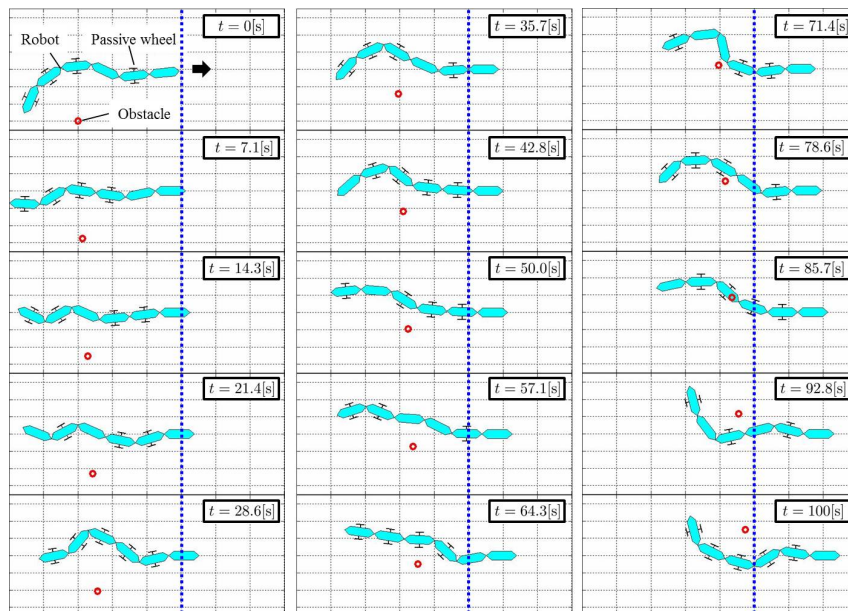


Figure 10. Motion of the robot with random switching in simulation.

4. Simulations

In this simulation, we consider a six-link snake robot where $l_f = l_b = l_g = 0.088$ m, $l_w = 0.043$ m and $N_m = 16$. The parameters are equal to those of the experimental snake robot to be described in the next section. Figure 8 shows the configurations of all modes of a six-link snake robot. We set the initial condition as $\mathbf{w}(0) = [-0.01, -0.01, 3.24]^T$ and $\phi(0) = [-\pi/6, \pi/6, \pi/6, \pi/6, \pi/6]^T$, the desired trajectory as $\mathbf{w}_d = [0.005t, 0, \pi]^T$, and the position of the moving obstacle as $(x_{ob}, y_{ob}) = (-0.6 + 0.0055t, -0.3 + 0.0045t)$, and define $K = 1$, $\Delta T = 2$ s, $k_n = -0.05$, $a = 10$, $b = 1.0$ and $c_s = 0.05$.

Figure 9 shows the motion of the snake robot and obstacle in the case that the mode is eight ($\sigma = 8$) without switching modes, while circles represent the position of the obstacle and the

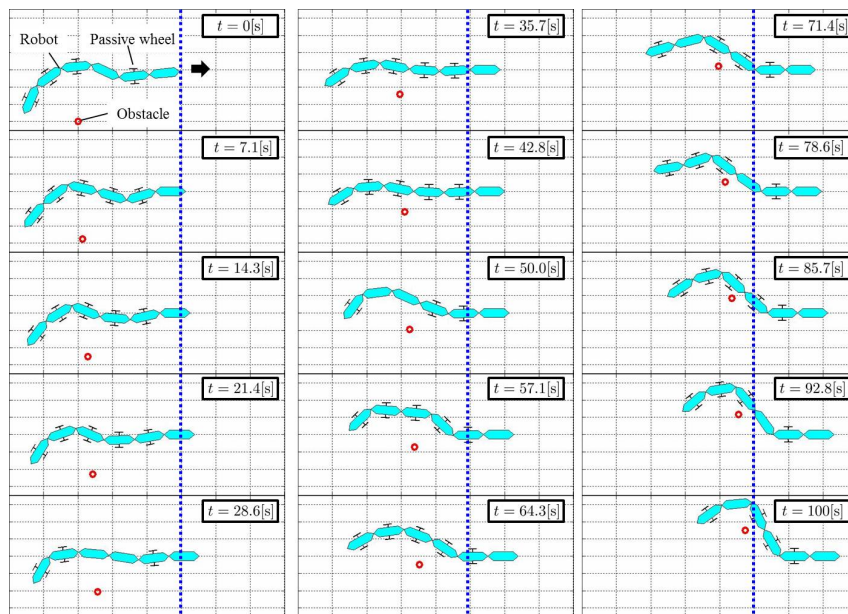


Figure 11. Motion of the robot with optimal switching in simulation.

lifted wheels are not drawn. The robot attempted to avoid the obstacle using redundancy until $t = 71.4$ s, but finally collided with the obstacle because the non-holonomic constraint of the wheel of the fourth link prevented the robot from avoiding the collision. Figure 9 corresponds to the result of our previous work [26], which investigated the control of snake robots without switching, and shows that the robot cannot avoid collision with a moving obstacle. Figure 10 shows the motion in the case of random switching. The robot collided with the obstacle at $t = 85.7$ s. Thus, it was found that there was a limit to the avoidance motion of the robot in the case without switching modes and the case with random switching.

Figures 11–15 show the simulation results for the case with optimal switching following (13). Figure 11 shows the motion of the robot and obstacle. Figures 12–15 show the time response and the desired trajectory of \mathbf{w} , and the time response of the angles ϕ , the input \mathbf{u} , modes σ , $\det \tilde{A}_\sigma^T \tilde{A}_\sigma$, $d_{min} = \min_{i \in \{1, \dots, n\}} d_i$, and the cost function V . The obstacle was moving to approach the body of the robot and the robot avoided the obstacle if the distance between the robot and obstacle became small as shown in Figure 11. The controlled variables \mathbf{w} tracked the desired trajectory as shown in Figure 12 and the singularity was avoided because of $\det \tilde{A}_\sigma^T \tilde{A}_\sigma \neq 0$ as shown in Figure 15. Therefore, it was found that the robot could accomplish trajectory tracking, singularity avoidance, and moving obstacle avoidance using the proposed controller with optimal switching.

5. Experiments

Experiments were carried out to determine the effectiveness of the proposed control strategy. The experimental system is shown in Figure 16. The snake robot has links on which the passive wheels and the pitch joints are mounted, and the links are connected by yaw joints, where $l_f = l_b = l_g = 0.088$ m, $l_w = 0.043$ m, and the diameter of the wheels is 0.058 m. The first link is wheelless. Actuators of the joints are Dynamixel MX-64R manufactured by ROBOTIS. Yaw joints are used for motion on the xy plane and correspond to ϕ_i in Figure 1. Pitch joints are used to switch constraints. Passive wheels and pitch joints are placed coaxially in each link. The real-time position and attitude of the robot's head and the position of the moving obstacle were measured by OptiTrack which is an optical motion capture system and tracking software manufactured by NaturalPoint, Inc. , and the real-time joint angles are measured by the absolute

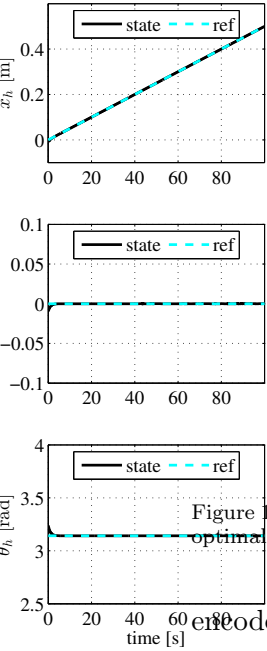


Figure 12. Time responses of w with optimal switching in simulation.

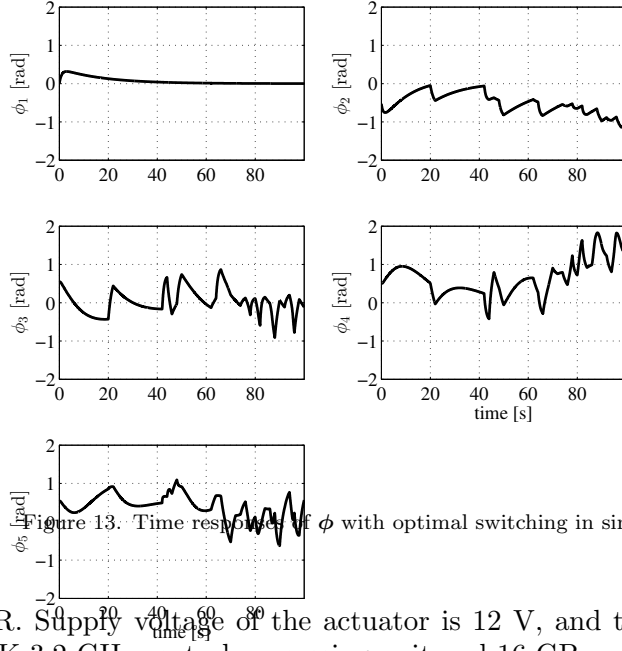


Figure 13. Time responses of ϕ with optimal switching in simulation.

encoder in the Dynamixel MX-64R. Supply voltage of the actuator is 12 V, and the personal computer (PC) has a Core i7-3930K 3.2-GHz central processing unit and 16 GB random access memory. The PC calculates the input and controls actuators of the robot according to the proposed controller using the values measured by actuators and the motion capture system. The PC and actuators are connected with a daisy chain via an RS485 interface.

5.1 Implementation of switching constraints

Switching constraint is obtained from the motion of pitch joints of each link. The snake robot can lift a wheel using pitch joints as shown in Figure 17. Figure 18 shows the model of a lifting motion of the snake robot. ψ_i is the angle of the pitch joint of the i -th link. The wheel of the i -th link can be lifted using the pitch joints of the $i, i-1, i+1$ -th links. ψ_{id} is the desired value of ψ_i . ψ_{id} is set as in Table 1 to switch constraints depending on the constraint conditions of the $i, i-1, i+1$ -th links where α is a minute value to ensure switching without adverse effects on motion in the xy plane. We set the angular velocity of the pitch joint $\dot{\psi}_i$ as:

$$\dot{\psi}_i = -K_P(\psi_i - \psi_{id}) - K_I \int (\psi_i - \psi_{id}) dt \quad (14)$$

where $K_P, K_I > 0$ are the feedback gain and (14) is a proportional-integral controller.

5.2 Experimental results

The initial condition $\phi(0)$, the desired trajectory w_d , and other parameters are equal to those in the simulations. We set $K_P = 4$, $K_I = 0.1$, and $\alpha = \pi/120$, and the obstacle is operated by human hands to approach the robot.

Figures 19–24 show the experimental results in the case with optimal switching following (13).

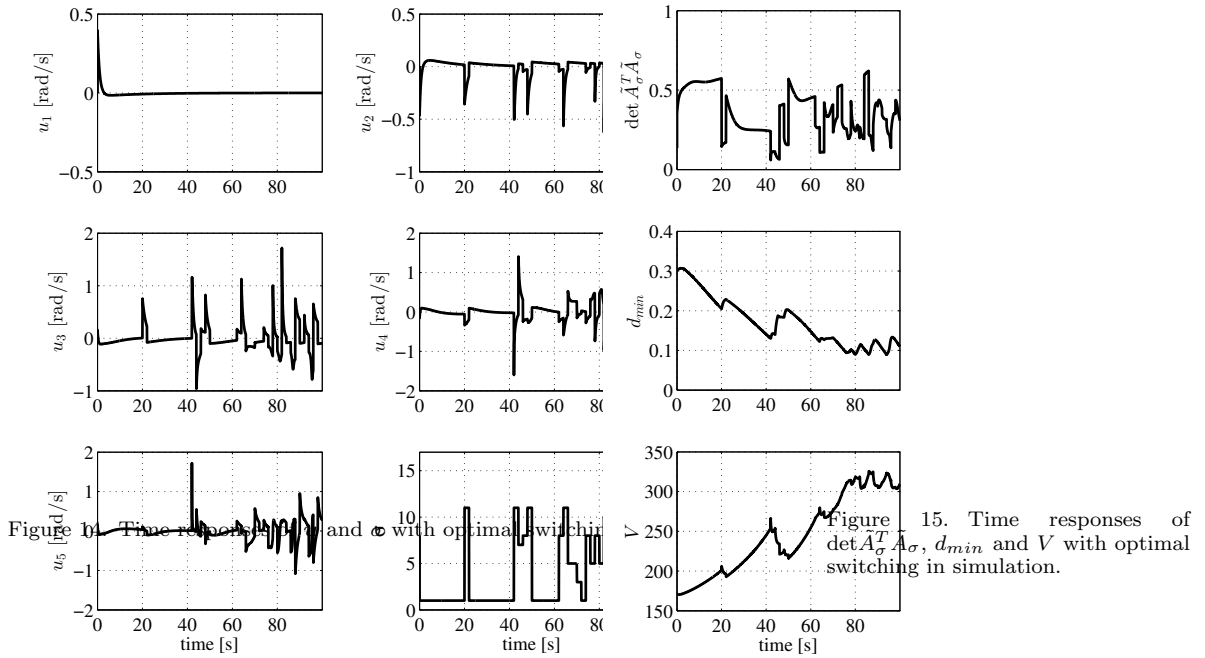


Figure 15. Time responses of $\det \tilde{A}_\sigma^T \tilde{A}_\sigma$, d_{min} and V with optimal switching in simulation.

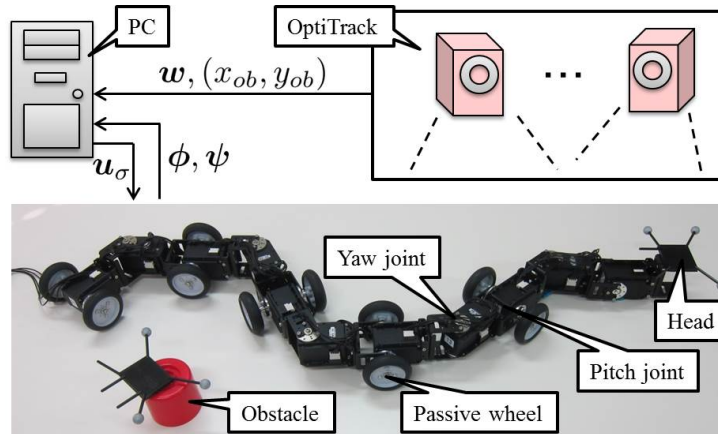


Figure 16. Experimental system.



Figure 17. An example of lifting motion of the snake robot by pitch joints.

Figures 19–23 show the time response and the desired trajectory of w , and the time responses of ϕ , ψ , u , σ , $\det \tilde{A}_\sigma^T \tilde{A}_\sigma$, d_{min} , and V . Figure 24 shows the motions of the robot and obstacle. The controlled variable w tracked the desired trajectory w_d as shown Figure 19 and the robot

Table 1. Constraint conditions and ψ_{id} .

| i -th link | $(i-1)$ -th link | $(i+1)$ -th link | ψ_{id} |
|--------------|------------------|------------------|-------------|
| grounded | lifting | lifting | 2α |
| | lifting | grounded | α |
| | grounded | lifting | α |
| | grounded | grounded | 0 |
| lifting | lifting | lifting | 0 |
| | lifting | grounded | $-\alpha$ |
| | grounded | lifting | $-\alpha$ |
| | grounded | grounded | -2α |

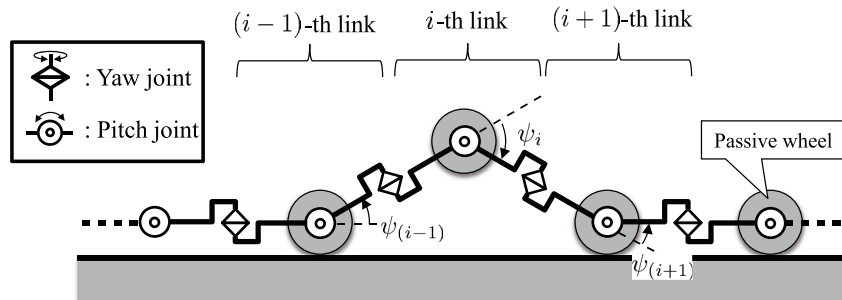


Figure 18. Model of a lifting motion by pitch joints.

avoided the singular configuration because $\det \tilde{A}_\sigma^T \tilde{A}_\sigma \neq 0$ as shown in Figure 23. It was found that the switching of modes was accomplished because the pitch angles ψ were close to the desired value. The obstacle was operated to move toward the body and d_{min} became smaller. d_{min} temporarily increased after the robot switched modes and moved to avoid the obstacle if d_{min} became some small value. In Figures 23 and 24, it was found that the mode was switched and motion was generated to avoid the obstacle if the obstacle came close to the body.

However, there was error of \mathbf{w} at $t = 41, 49, 65, 89, 96$ s. We guess that one of the causes of the error was the large acceleration because there were discontinuous changes in \mathbf{u} because of the switching of modes. The large acceleration generated the sideslip of a wheel. Moreover, from the start of the switching to the time when the pitch angle ψ reached the desired value took about 1 s, despite the assumption that the time to lift and ground wheels is infinitesimal. Hence, there was modeling error between the actual mode of the system and the mode that was used in calculation of the input. We need to consider the transition time taken to complete switching to realize more accurate tracking.

As a result, it was found that the snake robot can accomplish the trajectory tracking while avoiding the singular configuration and the moving obstacle using the proposed controller. The generated motion was a sideways motion of the body with the trajectory tracking of the robot's head. Sidewinding is known as a sideways motion of snake robots [10, 11, 16]. Previous studies [10, 11, 16] are different from ours in that they were inspired by real snakes and did not consider the tracking of the robot's head. The generated motion in this paper is effective and significant without regard to locomotion patterns of real snakes.

However, the increase in the number of links leads to a large increase in the calculation cost of the selection of the mode, and it is difficult to apply the proposed controller to a robot that has more than seven links. For example, if $n = 10$, N_m is 466 following (4), and the calculation cost is about 30 times that for $n = 6$. To reduce calculation cost is a goal of future works.

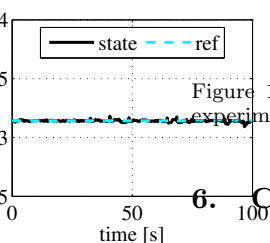
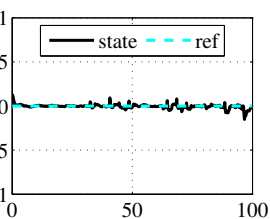
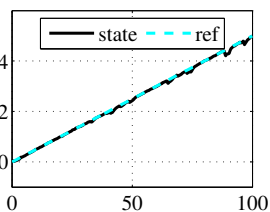


Figure 19. Time responses of w in experiment.

6. Conclusion

This paper presented a trajectory tracking controller of a snake robot with the switching of lifting parts. We derived the kinematic model of the motion of the snake robot with switching constraints, designed the controller to accomplish trajectory tracking, and proposed a method for selecting constraints to accomplish sub-tasks and switching conditions to ensure static stability and singularity avoidance of the robot. We introduced a cost function related to avoiding the singularity and moving obstacle for sub-tasks, and simulations and experiments were carried out to determine the effectiveness of the proposed controller and switching constraints. The snake robot accomplished trajectory tracking with moving-obstacle avoidance employing the proposed control method.

Further studies are required to improve the tracking accuracy by introducing the transition time of modes, decrease the calculation cost of selecting modes, and design the controller while planning the desired trajectory of the robot's head for more effective locomotion.

References

- [1] Arai M. Tanaka Y. Hirose S. Kuwahara H. Tsukui S. Development of "Souryu-IV" and Souryu-V:" serially connected crawler vehicles for in-rubble searching operations. *J. of Field Robotics*. 2008; 25:31-65.
- [2] Borenstein J. Hansen M. Borrell A. The omnitread OT-4 serpentine robot—design and performance. *J. of Field Robotics*. 2007; 24:601-621.
- [3] Liljeback P. Pettersen KY. Stavadahl O. Gravdahl JT. Hybrid modelling and control of obstacle-aided snake robot locomotion. *IEEE Trans. on Robotics*. 2010; 26:5:781-799.
- [4] Liljeback P. Pettersen KY. Stavadahl O. Gravdahl JT. Experimental investigation of obstacle-aided

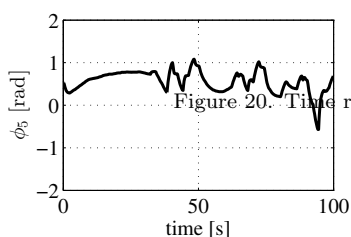
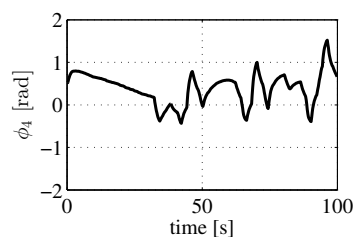
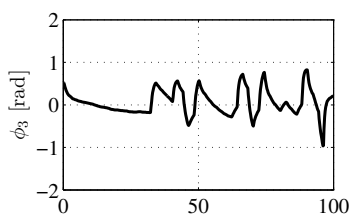
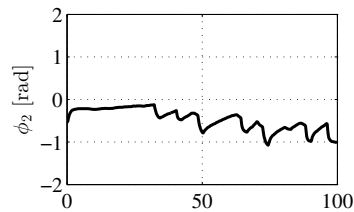
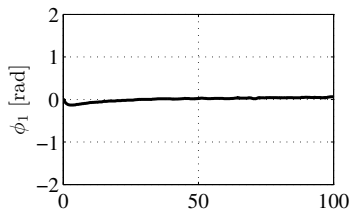


Figure 20. Time responses of ϕ in experiment.

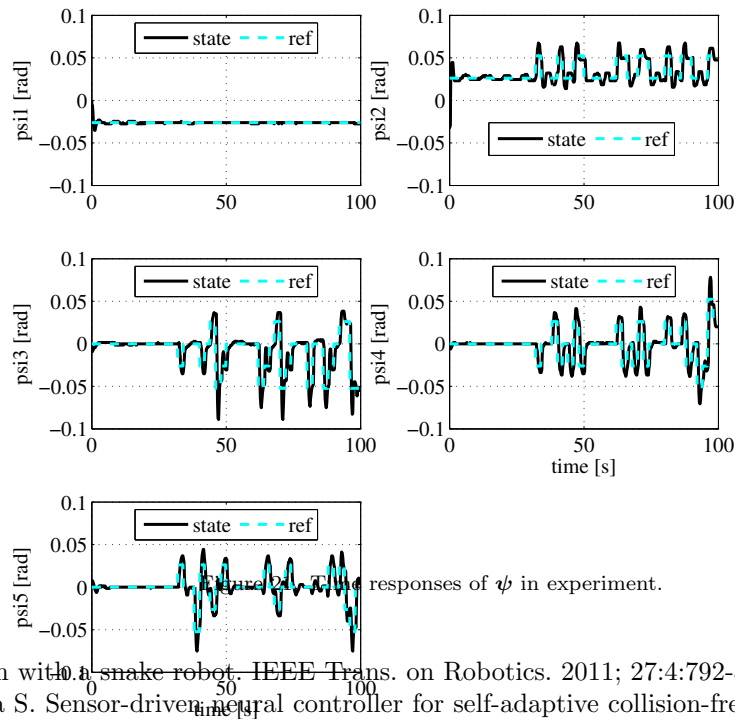
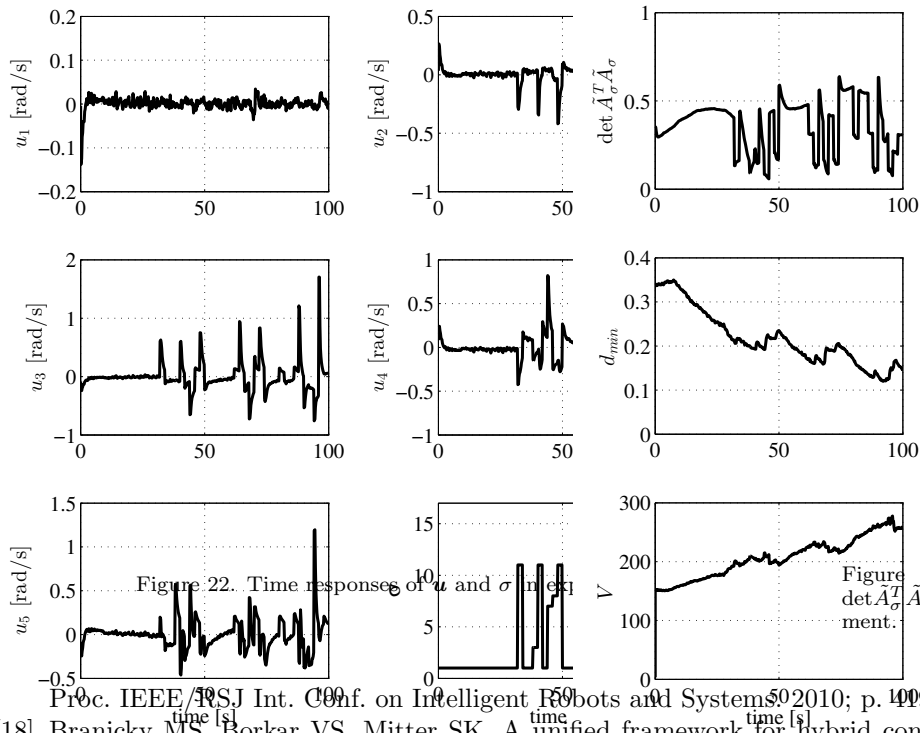
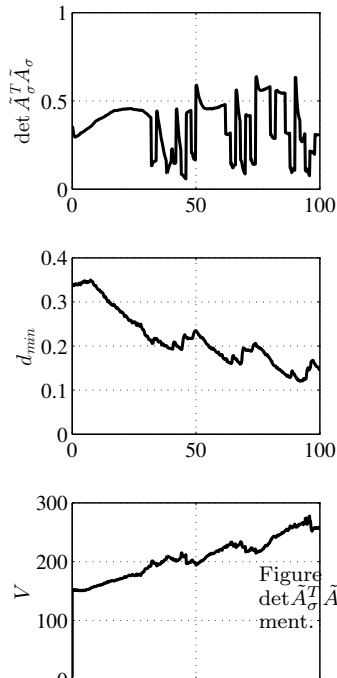


Figure 2: The responses of ψ in experiment.

- locomotion with a snake robot. *IEEE Trans. on Robotics*. 2011; 27:4:792-800.
- [5] Wu X. Ma S. Sensor-driven neural controller for self-adaptive collision-free behavior of a snake-like robot. *IEEE Int. Conf. on Robotics and Automation*. 2011; p. 191-196.
 - [6] Kamegawa T. Baba T. Gofuku A. V-shift control for snake robot moving the inside of a pipe with helical rolling motion. *Proc. IEEE Int. Symp. on Safety, Security and Rescue Robotics*. 2011; p.1-6.
 - [7] Sato T. Kano T. Ishiguro A. A snake-like robot driven by a decentralized control that enables both phasic and tonic control. *Proc. IEEE/RSJ Int. Conf. on Intelligent Robots and Systems*. 2011; p. 1881-1886.
 - [8] Hatton RL. Choset H. Optimizing coordinate choice for locomoting systems. *IEEE Int. Conf. on Robotics and Automation*. 2010; p. 4493-4498.
 - [9] Hirose S. *Biologically inspired robots (snake-like locomotor and manipulator)*. Oxford University Press. 1993.
 - [10] Burdick JW. Radford J. Chirikjian GS. A 'Sidewinding' locomotion gait for hyper-redundant robots. *Proc. IEEE Int. Conf. on Robotics and Automation*. 1993; p. 101-106.
 - [11] Hatton RL. Choset H. Sidewinding on slopes. *Proc. IEEE Int. Conf on Robotics and Automation*. 2010; p.691-696.
 - [12] Ma S. Ohmameuda Y. Inoue K. Dynamic analysis of 3-dimensional snake robots. *Proc. IEEE/RSJ Int. Conf. on Intelligent Robots and Systems*. 2004; p. 767-772.
 - [13] Shigeta K. Date H. Nakaura S. Sampei M. Improvement of manipulability for locomotion of a snake robot by mass distribution. *Proc. SICE Annual Conference 2002*. 2002; p. 2214-2217.
 - [14] Tsuda M. Nakaura S. Sampei M. Dynamic manipulability of a snake-like robot and its effect for sinus-lifting motion. *Proc. SICE Annual Conference 2004*. 2004; p. 2202-2207.
 - [15] Lipkin K. Brown I. Peck A. Choset H. Rembisz J. Gianfortoni P. Naaktgeboren A. Differentiable and piecewise differentiable gaits for snake robots. *Proc. IEEE/RSJ Int. Conf. on Intelligent Robots and Systems*. 2007; p. 1864-1869.
 - [16] Gong C. Hatton RL. Choset H. Conical sidewinding. *Proc. IEEE Int. Conf. on Robotics and Automation*. 2012; p. 4222-4227.
 - [17] Yamada H. Hirose S. Steering of pedal wave of a snake-like robot by superposition of curvatures.

Figure 22. Time responses of u and σ in experiment.Figure 23. Time responses of $\det \tilde{A}_\sigma^T \tilde{A}_\sigma$, d_{min} , and V in experiment.

- Proc. IEEE/RSJ Int. Conf. on Intelligent Robots and Systems, 2010; p. 409-424.
- [18] Branicky MS, Borkar VS, Mitter SK. A unified framework for hybrid control: model and optimal control theory. IEEE Trans. on Automatic Control. 1998; 43:1:31-45.
- [19] Liberzon D. Switching in systems and control. Boston: Birkhauser; 2003.
- [20] Tanaka M, Matsuno F. A study on sinus-lifting motion of a snake robot with switching constraints. Proc. IEEE Int. Conf. on Robotics and Automation; 2009; p. 2270-2275.
- [21] Toyoshima S, Matsuno F. A study on sinus-lifting motion of a snake robot with energetic efficiency. Proc. IEEE Int. Conf. on Robotics and Automation; 2012; p. 2673-2678.
- [22] Hasanzadeh S, Tootoonchi AA. Obstacle avoidance of snake robot moving with a novel gait using two-level PID controller. Proc. IEEE Int. Conf. on Robotics, Automation and Mechatronics. 2008; p.427-432.
- [23] Yagnik D, Ren J, Liscano R. Motion planning for multi-link robots using artificial potential fields and modified simulated annealing. Proc. IEEE/ASME Int. Conf. on Mechatronics and Embedded Systems and Applications. 2010; p.421-427.
- [24] Hitaka Y, Yokomichi M. Obstacle avoidance of a snake robot in narrow hallway. Proc. IEEE Int. Conf. on Mechatronics and Automation. 2012; p.214-219.
- [25] Wu X, Ma S. Newrally controlled steering for collision-free behavior of a snake robot. IEEE Trans. on Control Systems Technology. 2013; (Early access articles)
- [26] Matsuno F, Mogi K. Redundancy controllable system and control of snake robot with redundancy based on kinematic model. Proc. IEEE Conf. on Decision and Control; 2000; p.4791-4796.
- [27] Kamegawa T, Yamasaki T, Igarashi H, Matsuno F. Development of the snake-like rescue robot "KOHGA". Proc. IEEE Int. Conf. on Robotics and Automation; 2004; p. 5081-5086.
- [28] Yamada H, Takaoka S, Hirose S. A snake-like robot for real-world inspection applications (the design and control of a practical active cord mechanism). Advanced Robotics; 2013; 27:47-60.
- [29] Prautesch P, Mita T, Iwasaki T. Analysis and control of a gait of snake robot. Trans. IEE J. Ind. Appl. Soc; 2000; 120-D:372-381.
- [30] Nakamura Y, Hanafusa H, Yoshikawa T. Task-priority based redundancy control of robot manipu-

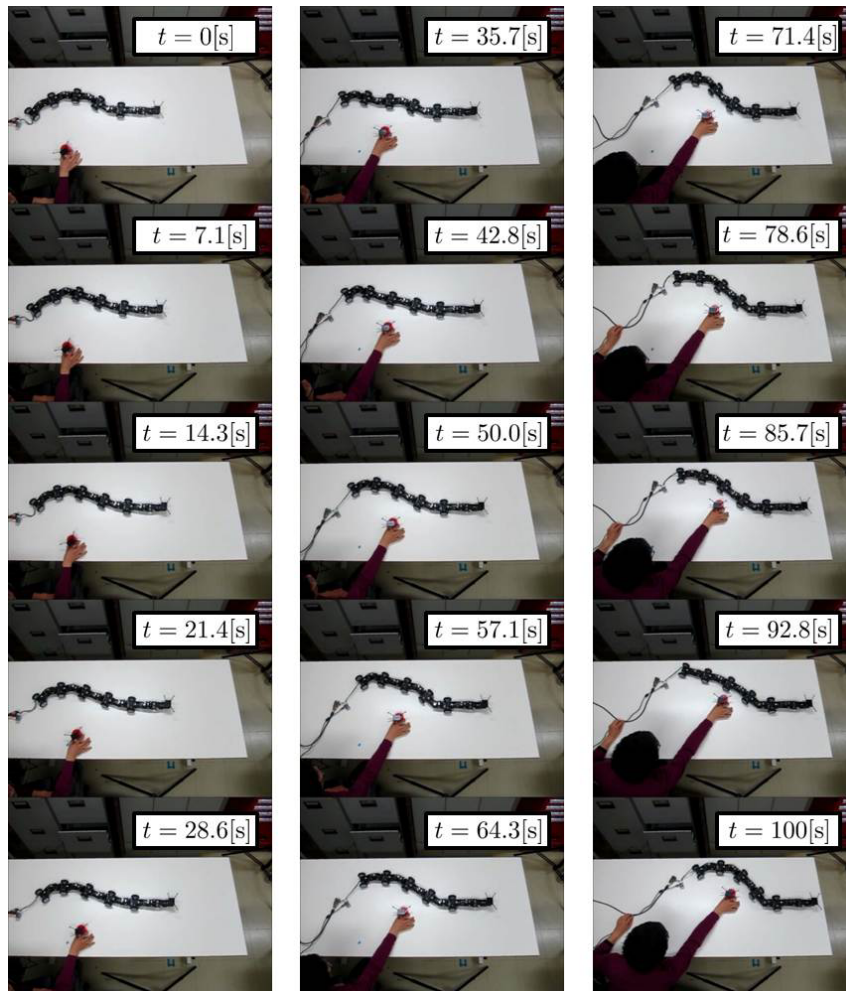


Figure 24. Motion of the robot in experiment.

lators. Int. J. of Robotics Research; 1987;6:2:3-15.